

## DEFORMATION AND DAMAGE OF Fe-Cr STEELS IN A WIDE TEMPERATURE RANGE

Vladimir A. Skripnyak<sup>1</sup>, Natalia V. Skripnyak<sup>1,2</sup>, Vladimir V. Skripnyak<sup>1(\*)</sup>, Evgeniya G. Skripnyak<sup>1</sup>

<sup>1</sup>National Research Tomsk State University (TSU), Lenin Avenue, 634050 Tomsk, Russia.

<sup>2</sup>Linköping University, 581 83 Linköping, Sweden

(\*)Email: skrp2012@yandex.ru.

### ABSTRACT

The deformation and damage of a high chromium steels in a wide temperature range was studied by numerical simulation method. A model was proposed to predict the deformation and damage of high chromium steels at a quasi-static loading within the temperature range from 295 K to 1100 K. The model takes into consideration mechanisms of hardening and softening high chromium steels in a wide temperature range. It is shown that the ductility of high-chromium steels increases proportional to temperature in the range from 750 K to 1100 K in connection with the growth of precipitates of  $\alpha'$ -phase.

**Keywords:** modelling, mechanical properties, elevated temperature, high chromium steel, damage, precipitation hardening,  $\alpha'$ -phase

### INTRODUCTION

High chromium steels, including oxide dispersion strengthened (ODS) grades are an important class of steels with a unique combination of properties - high resistance to aqueous corrosion, high temperature oxidation resistance, high strength and ductility, resistance against thermal creep, weldability, neutron irradiation hardening effect (El-Genk, 2005, Klueh, 2007, Samaras, 2007, Terentyev, 2010, Bonny, 2010). These steels are considered as structural material for critical components of Gen IV reactor. The study of the mechanical behavior of high chromium steels in a wide temperature range, including in combination with radiation and neutron radiation is intensively carried out using experimental methods and molecular dynamics method (Samaras, 2007, Terentyev, 2010, Barrett, 2014).

Terentyev showed the decomposition of high chromium steel into the Fe - rich  $\alpha$  and Cr-rich  $\alpha'$  - phases takes place under thermal aging (Terentyev, 2010). The fragment of Fe - Cr phase diagram steel is shown in Fig. 1. CR-rich  $\alpha'$  - phase is formed at temperatures higher than 748 K in the process of thermal ageing of high chromium steels (Bonnie, 2010). The formation of Cr - rich  $\alpha'$  - phase takes place under irradiation at temperature below the peak thermal aging temperature (753 K). This effect can be explained by the acceleration of the formation of  $\alpha'$  - phase due to the production of mobile point defects after the collision damage cascade (Samaras, 2007, Terentyev, 2010).

Thus, damage at elevated temperatures is an important impact factor on the mechanical behavior of high chromium steels. Precipitates of  $\alpha'$  - and  $\sigma$  - phases causes the hardening effect of Fe - Cr steel due to pinning dislocations.

The yield strength decreases in the range from 473 K to 1073 K due to reduction of the mole fraction of precipitates of the  $\alpha'$ - and  $\sigma$  - phases with increasing temperature K (Samaras, 2007).

Relaxation of the shear stress in high chromium steel is caused by a combination of multiple mechanisms of interaction of dislocations with grain boundaries, boundaries of  $\alpha$  - and  $\sigma$  - phases, oxide, carbide nanoparticles, and defects (Terentyev, 2013, Barrett, 2014).

The  $\alpha'$ -phase is observed to form finely dispersed precipitates in the bulk and does not appear to be associated with radiation defects.

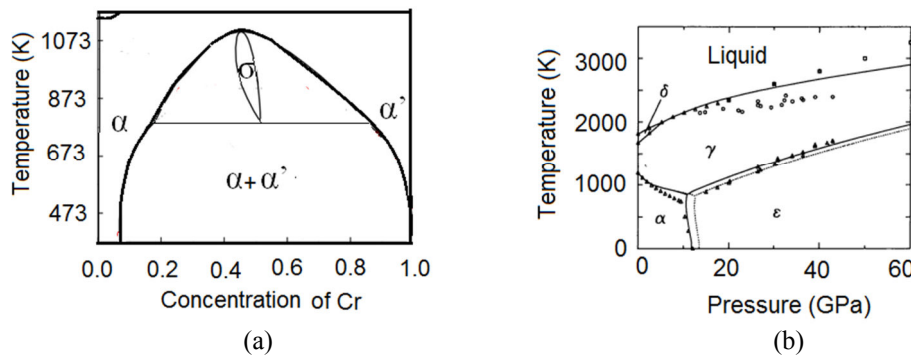


Fig. 1 - Fe-Cr phase diagram (a) (Bonny, 2010), and the phase diagram of Fe-Cr steel (b) (Kerley, 1993)

The aim of this work is predicting the deformation and damage of Fe-Cr steels in a wide temperature range up to 1100 K.

## DESCRIPTION OF THE MODEL

Mechanical behavior at the macroscopic level is described by a system of conservation equations (the kinematic equations, equations of conservation of mass, momentum and energy), and the constitutive equation in which the relaxation of the shear stress is calculated by the dislocation model of plastic flow.

The constitutive equation is used in the form

$$\sigma_{ij} = \sigma_{ij}^{(m)} (1 - D), \quad \sigma_{ij}^{(m)} = -p^{(m)} \delta_{ij} + S_{ij}^{(m)}, \quad (1)$$

where  $D$  is the damage parameter,  $\sigma_{ij}$  is the stress tensor components,  $p$  is the pressure, and  $S_{ij}$  stress deviator components, respectively,  $\delta_{ij}$  is the Kronecker delta, the superscript  $m$  indicates an undamaged phase.

The equation of state for condensed  $\alpha$ ,  $\gamma$  and  $\epsilon$  phases of Fe-Cr steels is used

$$p(\rho, T) = p_x(\rho) + \gamma(\rho) \rho E_T, \quad (2)$$

$$p_x^{(m)} = \frac{3}{2} \cdot B_0 \cdot (\xi^{-7/3} - \xi^{-5/3}) \cdot \left(1 - \frac{3}{4} (4 - B_1) \cdot (\xi^{-2/3} - 1)\right),$$

where  $\xi = \rho/\rho_0$ ,  $\rho_0$ ,  $\gamma(\rho) = (\gamma_R - 0.5)(\rho_R / \rho) n - 0.5$ ,  $\gamma_R$ ,  $\rho_R$ ,  $n$ ,  $B_0$ ,  $B_1$  are the material constants given in Table 1 (Bonny, 2010, Kerley, 1993).

The density of Fe-Cr steel consisting of a mixture of phases was calculated by relation

$$\rho(T) = \sum_{k=1}^3 \rho_k(T) C_k(T) \quad (3)$$

where  $T$  is the temperature,  $C_k(T)$  is the mass fraction of phase  $k$ ,  $\rho_k(t)$  is the mass density of phase  $k$  ( $\alpha$ ,  $\gamma$  and  $\epsilon$  phases).

$C_k(T)$  calculated using by phase diagrams shown in Fig. 1a,b.

Table 1 - The parameters of the solid phases in Fe-Cr steels

Parameter	$\alpha$ -phase	$\gamma$ -phase	$\epsilon$ -phase
$\rho_0$ , g/cm <sup>3</sup>	7.969	8.060	8.430
$B_0$ , GPa	173.0	174.0	182.0
$B_1$	4.8	4.7	5.00
$\gamma_R$	1.7	1.65	2.40
$\rho_R$ , g/cm <sup>3</sup>	7.873	7.953	8.264
$n$	1	1	2

$$E_T = C_p T, \quad (4)$$

where  $T$  is temperature and  $C_p$  is the specific heat capacity of phases.

The ideal mixture model assumes

$$C_p = \sum_{k=1}^3 C_{pk}(T, p) \xi_k, \quad (5)$$

where  $C_{pk}$  is the specific heat capacity of  $k$ -phase,  $\xi_k$  is the molar fraction of  $k$ -phase.

The specific heat capacity for Fe-Cr steel can be calculated by the phenomenological relations within temperature range from 293 to 1115 K (Su,2016)

$$\begin{aligned} C_p &= 0.4251 - 2.784e^{-4}T + 1.197e^{-6}T^2 \text{ at } 293K < T < 1023K \\ C_p &= 23.8935 - 0.05375T + 3.0899e^{-5}T^2 \text{ at } 1023K < T < 1115K, \end{aligned} \quad (6)$$

The components of the strain rate tensor  $\dot{\varepsilon}_{ij}$  are determined by relation

$$\dot{\varepsilon}_{ij} = \frac{1}{2} (\nabla_i u_j + \nabla_j u_i), \quad (7)$$

where  $u_i$  is components of the material particle velocity, and  $\nabla_i$  is an operator nabla.

$$\dot{\varepsilon}_{ij} = \frac{1}{3} \dot{\theta} \delta_{ij} + \dot{e}_{ij}, \quad (8)$$

where  $\dot{\theta} = \dot{\varepsilon}_{kk}$  is the bulk strain rate,  $\dot{e}_{ij}$  is the deviator of the strain rate tensor.

The deviator of stress tensor is calculated by the equation

$$dS^{(m)}_{ij} / dt = 2\mu(\dot{e}_{ij} - \dot{e}_{ij}^p), \quad (9)$$

where  $d/dt$  is the Jaumann's derivative,  $\mu$  is the shear modulus, and  $\dot{e}_{ij}^p$  is the deviator of the inelastic strain rate tensor.

The shear modulus and the Poisson ratio at temperature T calculated by the Hashin -Strikman bound (Talbot, 1995). The shear modulus of solid phase were calculated by relation

$$\mu_k(T) = \mu_{0k}^c (1 - \alpha_d) [1 + A_{sk} p - B_{sk} (T/T_m - 297 K/T_m)], \quad (10)$$

where  $\mu_{0k}^c$  is the shear modulus of a k-solid phase,  $A_{sk}$  and  $B_{sk}$  are the constants for a k-solid phase, and  $T_m$  is the melting temperature of Fe-Cr system.

Poisson's ratio can be described by the relation

$$v_k(T) = v_{0k} + k_v T + k_T p, \quad (11)$$

where  $v_k$  is the Poisson's ratio of k-phase,  $v_0$ ,  $k_v$ , and  $k_T$  are the k-phase constants. We use  $v_0=0.29$  and  $k_p=0.0008$  for the  $\alpha$ -phase of Fe-Cr steel.

The temperature dependence of the bulk modulus  $B_{0k}(T)$  of k-phase can be calculated as

$$B_{0k}(T) = \frac{2\mu_k(T)(1+v_k(T))}{3(1-2v_k(T))}. \quad (12)$$

The damage parameter is calculated by Eq. (2)

$$D = \frac{1}{C_1} \int_0^{e_{eq}^p} \left\{ \exp\left(-\frac{p}{\sigma_{eq}} C_2\right) / \left[1 - C_3 \frac{T - T_s^{\alpha'}}{T_f^{\alpha'} - T_s^{\alpha'}} H(T_f^{\alpha'} - T) H(T - T_s^{\alpha'})\right] \right\} d\epsilon_{eq}^p, \quad (13)$$

where D is the damage parameter,  $\epsilon_{eq}^p = [(2/3)\epsilon_{ij}^p \epsilon_{ij}^p]^{1/2}$ ,  $C_1$ ,  $C_2$ , and  $C_3$  are the material parameters,  $\sigma_{eq} = [1.5 S_{ij} S_{ij}]^{1/2}$ ,  $p$  is the pressure,  $T$  is temperature,  $T_s^{\alpha'} - T_f^{\alpha'}$  is the temperature range in which there is  $\alpha'$  - phase,  $H(.)$  is the Heaviside function, and  $\frac{p}{\sigma_{eq}}$  is the triaxiality stress factor (Kacker, 2015).

The damage accumulation at the temperature can be represented by a general law that accounts for both the growth of defects and nucleation new damages (microcracks or voids).

The local damage of material particles described by criterion

$$D = 1. \quad (14)$$

The yield criterion is used in the form

$$\sigma_{eq} \leq \sigma_s, \quad (15)$$

where  $\sigma_s$  is the yield strength.

The deviator of the inelastic strain rate tensor is determined be relation

$$\dot{\epsilon}_{ij}^p = (3/2)[S_{ij} \dot{\epsilon}_{eq}^p / \sigma_{eq}]. \quad (16)$$

The scalar function  $\dot{\epsilon}_{eq}^{p(m)}$  is defined as sum of parts corresponded to dislocation movements and dislocation nucleation near precipitates (Skripnyak, 2016)

$$\dot{\epsilon}_{eq}^p = [\dot{\epsilon}_{eq}^p]_{disl} + [\dot{\epsilon}_{eq}^p]_{disl\_nucle}, \quad (17)$$

where  $[\dot{\epsilon}_{eq}^p]_{disl}$  and  $[\dot{\epsilon}_{eq}^p]_{disl\_nucle}$  are the inelastic strain rates caused by dislocation movement and dislocation nucleation, respectively.

The inelastic strain rate due to dislocation movements can be described by relation (Skripnyak, 2016)

$$[\dot{\epsilon}_{eq}^p]_{disl} = g b v N_m \exp(-\Delta G_1 / kT), \quad (18)$$

where  $g \sim 0.5$  is the orientation coefficient,  $b$  is the modulus of the Burgers vector,  $b$  ( $\alpha$ -phase)  $\sim 0.248$  nm,  $v$  is the mean dislocation velocity,  $N_m$  is the mobile dislocation density,  $k$  is the Boltzmann constant,  $\Delta G_1 = \Delta G_0 [1 - (\sigma_{eq} / \sigma_{eq}^*)^{n_1}]^q$  is the activation energy for slip systems,  $\Delta G_0 \approx 0.35 \mu b^3$ ,  $n_1 \approx 0.28$ , and  $q \approx 1.34$  (Alsabbagh, 2014).

The inelastic strain rate due to heterogeneous dislocation nucleation described by relation (Skripnyak, 2016)

$$[\dot{\epsilon}_{eq}^p]_{disl\_nucle} = g b \dot{N}_{nucle} l_0 \exp(-\Delta G_2 / kT) \quad (19)$$

where  $\dot{N}_{nucle}$  the rate of growth of density of dislocations under nucleation is,  $l_0$  is the average size of dislocation loops,  $\Delta G_2$  is the activation energy of nucleation.

$$\dot{N}_{nucle} = (p + (2/3)\sigma_{eq})^4 H[p + (2/3)\sigma_{eq} - \sigma^*], \quad N_{nucle} = \int_0^t \dot{N}_{nucle} dt, \quad (20)$$

where  $\sigma^*$  is the threshold stress of the heterogeneous nucleation of dislocations,  $H(.)$  is the Heaviside function.

The evolution of mobile dislocation density includes both growth and reduction. The mobile dislocation density is described by the relation

$$N_m = N[f^* + (f^* - f_0) \exp(-k_1 \epsilon_{eq}^p \frac{1 - N_m}{N^*})], \quad (21)$$

$$N = N^* + (N_0 - N^*) \exp(-A \epsilon_{eq}^p)$$

where  $N_0$ ,  $N^* \sim 2 \cdot 10^{11} \text{ cm}^{-2}$  (Terentyev, 2010, 2013) are the initial dislocation density, equilibrium dislocation density under dislocation generation and annihilation, respectively,  $A$  and  $k_1$  are the material constants,  $f_0$  and  $f^*$  are the initial and equilibrium parts of mobile dislocations.

The average velocity of dislocation is described by relation

$$v = \sigma_{eff} b / B_v, \quad (22)$$

where  $\sigma_{eff}$  is the critical resolved shear stress on the slip system,  $B_v = Bv_0 / [1 - (v/c_s)2]$  is the damping coefficient,  $Bv_0$  is the nominal value of the damping coefficient, and  $c_s = (\mu/\rho)^{1/2}$  is the shear sound velocity (Austin, 2010).

Small Cr clusters and Cr-rich precipitates formed above the solubility limit do provide obstacles to dislocation glide (Yang, 2014). Mechanisms of interaction between dislocations and radiation-produced defects, such as voids and dislocation loops, are the same in Fe and Fe-Cr alloys (Terentyev, 2013).

The critical resolved shear stress on the slip system is given as

$$\sigma_{\text{eff}} = \sigma_{\text{eq}} - \sigma_{\text{GB}} - \sigma_{\text{bspr}} - \sigma_{\text{dn}} - \sigma_{\text{id}}, \quad (23)$$

where  $\sigma_{\text{GB}} = k_{\text{HP}} d_g^{-1/2}$  is the part of hardening effect caused by dislocation interaction at the grain boundary,  $\sigma_{\text{bspr}}$  is the back-stress caused by the presence of the various precipitates, and  $d_g$  is the grain size,  $\sigma_{\text{dn}} = k_2 \mu b(N)^{1/2}$  is the part of hardening effect due to dislocation substructure creation,  $\sigma_{\text{id}} = \mu b k_3 (N_{\text{irr}} d_{\text{irr}})$  is a part of hardening effect caused by irradiation-induced defects,  $b = 0.248$  nm is the magnitude of the Burgers vector,  $N_{\text{irr}}$  is the radiation-induced defect density, and  $d_{\text{irr}}$  is the defect diameter,  $k_{\text{HP}}$ ,  $k_2$ ,  $k_3$ , are the material constants, (Field, 2015).

Using Orowan-Ashby model  $\sigma_{\text{bspr}}$  can be calculated by the relation (Alsabbagh, 2014)

$$\sigma_{\text{bspr}} = 0.83 \mu b M \ln(r_s / 2b) / [(2\pi r_s \sqrt{1-v})(\sqrt{\pi/f_c} - 2)], \quad (24)$$

where  $\mu$  is the shear modulus of the  $\alpha$ -phase matrix ( $\sim 78$  GPa),  $v$  is the Poisson's ratio ( $\sim 0.33$ ),  $M \approx 3.06$  is Taylor factor,  $r_s$  is the average radius of cross section of Cr-rich clusters,  $f_c \approx 6.7 \cdot 10^{23} \text{ m}^{-3}$  is a density of Cr - rich clusters.

It was assumed that

$$r_s = r_s|_{t=0} + \int_0^t v_0 (T - T_s^{\alpha'}) H(T - T_s^{\alpha'}) H(T_f^{\alpha'} - T) dt, \quad (25)$$

where  $T$  is temperature,  $T_s^{\alpha'} = 748\text{K}$ ,  $T_f^{\alpha'} = 1115\text{K}$ ,  $H(.)$  is the Heaviside function,  $r_s|_{t=0}$  is an initial value of  $r_s$ ,  $t$  is a time.

The Eq. (23) determines the dependence of yield strength on temperature. The Dependence of plastic strain rate on the temperature is described by Eq. (18).

Eq. (13) predicts the damage of material during plastic flow. The Eq. (21) determines the dependence of yield strength on temperature.

The average grain size of the phases at a temperature  $T$  was calculated by the equation

$$d_g = d_{g0} \exp(k_2 t) \exp(-Q / 4RT), \quad (26)$$

where  $d_{g0}$  is the average grain size in steel,  $t$  is the residence time of the material at temperature  $T$ ,  $T$  is the absolute temperature in Kelvin,  $Q$  is the activation energy ( $\text{K J mol}^{-1}$ )  $R = 8.314 \text{ J K}^{-1} \text{ mol}^{-1}$  is the universal gas constant,  $k_2$  is the material constant.

Eq. (26) was obtained under the assumption on the implementation of an Arrhenius type equation of evolution grain sizes under annealing (Barrett, 2014).

Formation of  $\alpha'$  precipitates due to clustering and segregation Cr atoms under thermal heating and irradiation have stochastic nature.

Constitutive equation was used to predict the yield strength of high chromium steels under deformation in a wide range of temperature. We simulated mechanical behaviour of 9Cr-1MoV, Fe-14Cr-3W-0.4Ti-0.18O (14WT), Fe-14Cr-3W-0.4Ti-0.3Y-0.18O (14YWT) high chromium steels. The difference between the values of the yield strength of 14WT and 14YWT steels was caused by the concentration of nanoscale inclusions of  $\text{Y}_2\text{O}_3$  in 14YWTsteel (Nanstad, 2009).

## RESULTS

The calculated curve of the yield strength versus temperature is shown in Fig. 2. The experimental data for Fe-Cr steel are denoted by symbols (Nanstad, 2009). Curves 1,2,3 correspond to 14YWT, 14WT, and 9Cr-1MoV, respectively.

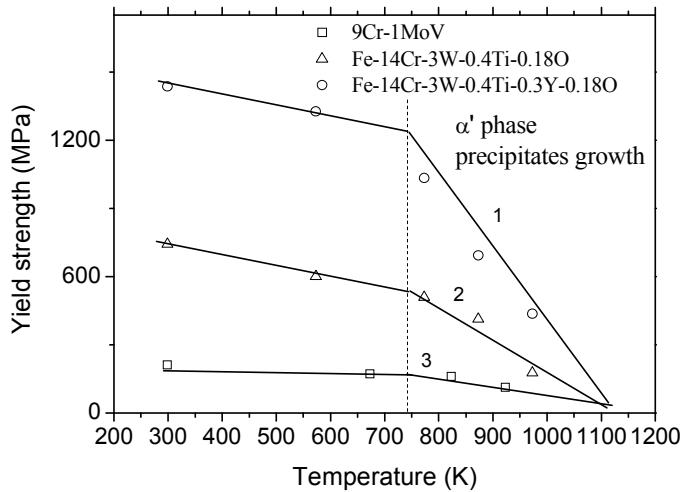


Fig. 2 - Calculated yield strength versus temperature, symbols are displayed experimental data (Nanstad, 2009)

It was assumed Fe-Cr steel the  $\alpha'$ -phase concentration increased within the temperature range from 750 to 1115 K. Recently, Yang has shown this effect for Fe-14% Cr steel (Yang 2014). Therefore, the volume fraction of the Cr-rich cluster  $f_c$  in Eq. (24) will depend on only the temperature.

In the calculations it was assumed that the steel has been heated to the temperature  $T$  and kept at this temperature until the formation of the average equilibrium particle size  $r_s$  of the  $\alpha'$ -phase.

Curve 1 and 2 corresponds to 14WT and 14YWT. The simulation results showed close values of the softening of these steels in the range from 295 K to 750 K. The softening of 9Cr-1MoV steel is less than for 14WT and 14YWT, as the value of the yield strength.

Thus, the simulation results indicate that the high chromium steels have similar mechanisms of plastic deformation in the temperature range from 297 K to 750 K. This prediction agrees with experimental results by Praud et al. (Praud, 2012).

The softening of all considered high chromium steels are increased in the temperature range from 750 K to 1100 K. In the model this effect is due to increase of dislocation mobility nucleated around the inclusions. This conclusion correlates with results of Bachhav et al. (Bachhav, 2014).

It can be assumed that the increase in particle size of  $\alpha'$  phase under irradiation can reduce the effect of thermal softening below 750 K. The effect of irradiation-accelerated precipitation of  $\alpha'$ - phase in the high chromium steels is introduced into Eq. (23) of the model. However, the predicted irradiation hardening is insufficient at the temperature above 750 K.

Fig 3 showed the calculated strain to fracture versus temperature. Curve 1-2 corresponds to 14YWT. Curves 3-4 and 5-6 were calculated for 14WT and 9Cr-1MoV respectively. Values of the parameter  $C_3$  in the Eq. (13) were taken equal to 0.8, 0.95, and 1.1 for 14YWT, 14WT

and 9Cr-1MoV steels, respectively. The strain to fracture of all considered high chromium steels increased at temperature above 750 K. The slope of the lines is changed when the temperature exceeds 750 K. The size of  $\alpha'$ - phase (Cr-clusters) at the same duration of heating increases the proportionally temperature.

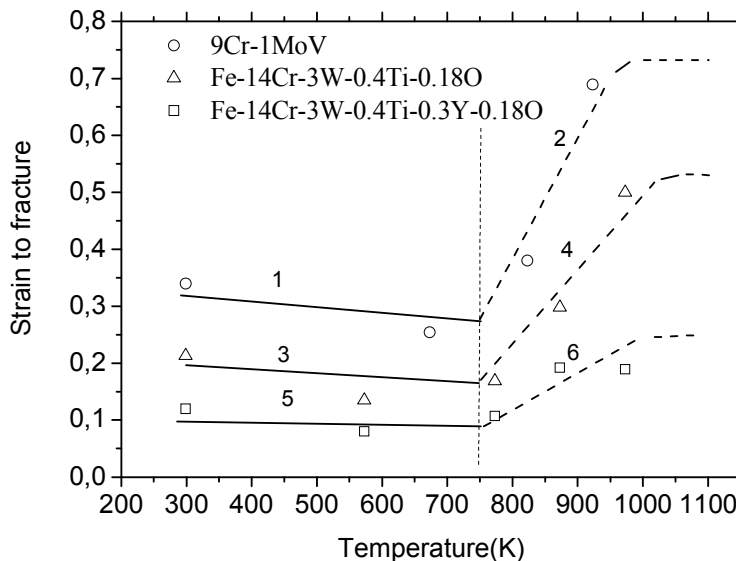


Fig. 3 - Calculated strain to fracture versus temperature, symbols are displayed experimental data (Nanstad, 2009)

The calculated values of strain to failure of high chromium steels increases proportional to the growth temperature in the range from 750 K to 1100 K. These results allow us to predict the delay of damage of high chromium steels under a quasi-static tensile at temperatures from 750 K to 1100 K.

## CONCLUSION

The multiscale approach was used to predict the mechanical behavior of precipitation-hardened 9Cr-1MoV, Fe-14Cr-3W-0.4Ti-0.18O (14WT), Fe-14Cr-3W-0.4Ti-0.3Y-0.18O (14YWT) high chromium steels in the temperature range up to 1100 K under a quasi-static loading.

A model was proposed to predict the deformation and damage of high chromium steels at a quasi-static loading at temperature range from 295 K to 1100 K.

The values of yield strength of high chromium steels decreases faster with increasing temperature in the range from 750 K To 1115 K than in the range from 295 K To 750 K. This effect is associated with the growth of  $\alpha'$  phase precipitates.

The ductility of high chromium steels increases proportional to temperature in the range from 750 K to 1100 K.

The increasing of the average size of  $\alpha'$  phase precipitates under irradiation can reduce the effect of thermal softening below 750 K. The softening of high chromium steels are increased in the temperature range from 750 K to 1100 K.

## ACKNOWLEDGMENTS

This work was supported partially by the Grant from the President of Russian Federation MK-2690.2017.8, CII-1916.2015.2. The authors are grateful for the support of this research.

## REFERENCES

- [1]-Alsabbagh A., Sarkar A., Miller B. at al., Microstructure and mechanical behavior of neutron irradiated ultrafine grained ferritic steel, Mater. Sci. Eng. A, 2014, 615, p.128-138.
- [2]-Austin R. A., and McDowell D. L., A dislocation-based constitutive model for viscoplastic deformation of FCC metals at very high strain rates, Int. J. Plasticity, 2010, 27, p. 1-24.
- [3]-Bachhav M., Odette G. R., and Marquis E. A.,  $\alpha'$  precipitation in neutron-irradiated Fe-Cr alloys, Scripta Materialia, 2014, 74, p. 48-51.
- [4]-Barrett R.A., O'Donoghue P.E., and Leen S.B. A dislocation-based model for high temperature cyclic viscoplasticity of 9-12Cr steels, Computational Materials Science, 2014, 92, p. 286-297.
- [5]-Bonny G., Terentyev D., and Malerba L., New contribution to the thermodynamics of Fe-Cr alloys as base for ferritic steels, J. Phase Equilib. Diff., 2010, 31, p. 439-444.
- [6]-El-Genk M.S., and Tournier J.-M., A review of refractory metal alloys and mechanically alloyed-oxide dispersion strengthened steels for space nuclear power systems, Journal of Nuclear Materials, 2005, 340, p. 93-112.
- [7]-Field K.G., Hu X., Littrell K. C., et al., Radiation tolerance of neutron-irradiated model Fe-Cr-Al alloys, Journal of Nuclear Materials, 2015, 465, p. 746-755.
- [8]-Kacker I., Bhaduria S.S., and Parashar V. Effect of strain ratio on stress triaxiality subjected to mode I fracture, International Journal of Mechanical and Production Engineering, 2015, 3, p. 2320-2092.
- [9]-Kerley G. I., Multiphase Equation of State for Iron, SANDIA, Report SAND93-0027 1 UC-41O Unlimited Release, 1993.
- [10]-Klueh R. L., and Nelson A. T., Ferritic/martensitic steels for next-generation reactors, Journal of Nuclear Materials, 2007, 371, p. 37-52.
- [11]-Nanstad R.K., McClintock D.A., Hoelzer D.T., Tan L., Allen T.R., High temperature irradiation effects in selected Generation IV structural alloys, Journal of Nuclear Materials 2009, 392, p. 331-340.
- [12]-Praud M., Mompiou F., Malaplate J., et al. Study of the deformation mechanisms in a Fe-14% Cr ODS alloy, Journal of Nuclear Materials, 2012, 428, p. 90-97.
- [13]-Samaras M., Hoffelner W., and M. Victoria, Modelling of advanced structural materials for GEN IV reactors, Journal of Nuclear Materials, 2007, 371, p. 28-36.

[14]-Skripnyak V. A., Emelyanova E. S., Sergeev M. V., Skripnyak N. V., and Zinovieva O. S. Strength and plasticity of Fe-Cr alloys, AIP Conference Proceedings, 2016, 1783, 020208. doi: 10.1063/1.4966502.

[15]-Su X., Wang G., Li J. et al., Dynamic mechanical response and a constitutive model of Fe-based high temperature alloy at high temperatures and strain rates, Springer Plus, 2016, 5, p.504-528.

[16]-Talbot D. R. S., Willis J.R., and Nesi V. On improving the Hashin-Shtrikman bounds for the effective properties of three-phase composite media, IMA J. Appl. Math, 1995, 54 (1) p. 97-107.

[17]-Terentyev D., Bonny G., Domain C., Monnet G., and Malerba L., Mechanisms of radiation strengthening in Fe-Cr alloys as revealed by atomistic studies, Journal of Nuclear Materials, 2013, 442, p. 470-485.

[18]-Terentyev D., Haghigat S. M. H., and Schäublin R., Strengthening due to Cr-rich precipitates in Fe-Cr alloys: Effect of temperature and precipitate composition, Journal of Applied Physics 2010, 107, 061806.

[19]-Yang Y. and Busby J. T., Thermodynamic modelling and kinetics simulation of precipitate phases in AISI 316 stainless steels, Journal of Nuclear Materials, 2014, 448, p.282-293.